



Engineering arbitrarily oriented spatiotemporal optical vortices using transmission nodal lines: supplement

HAIWEN WANG,¹  CHENG GUO,¹  WEILIANG JIN,² ALEX Y. SONG,²  AND SHANHUI FAN^{2,*} 

¹Department of Applied Physics, Ginzton Laboratory, Stanford University, Stanford, California 94305, USA

²Department of Electrical Engineering, Ginzton Laboratory, Stanford University, Stanford, California 94305, USA

*Corresponding author: shanhui@stanford.edu

This supplement published with The Optical Society on 25 June 2021 by The Authors under the terms of the [Creative Commons Attribution 4.0 License](https://creativecommons.org/licenses/by/4.0/) in the format provided by the authors and unedited. Further distribution of this work must maintain attribution to the author(s) and the published article's title, journal citation, and DOI.

Supplement DOI: <https://doi.org/10.6084/m9.figshare.14688834>

Parent Article DOI: <https://doi.org/10.1364/OPTICA.426460>

Generation of tilted spatiotemporal optical vortices using transmission nodal line: supplemental document

1. OAM IN SPATIOTEMPORAL PULSES

Throughout the paper, paraxial approximation and the slowly varying envelop approximation are assumed and the polarization of the pulses are assumed to be homogeneous. This allows us to describe the optical pulse using its envelope $E(x, y, z, t)$ which is a complex scalar. The real fields are given by $E_r = \text{Re}(Ee^{i\omega_0 t - k_0 z})$. Here $k_0 = \omega_0/c$. The total angular momentum of the pulse is given by [1]:

$$\mathbf{L} = \frac{1}{\mu_0 c^2} \int \mathbf{r} \times (\mathbf{E} \times \mathbf{B}) d^3 r \quad (\text{S1})$$

and can be decomposed into the spin part:

$$\mathbf{L}_{spin} = \frac{1}{\mu_0 c^2} \int \mathbf{E} \times \mathbf{A} d^3 r \quad (\text{S2})$$

and the orbital angular momentum part:

$$\mathbf{L}_{OAM} = \frac{1}{\mu_0 c^2} \int \sum_{j=1}^3 E_j (\mathbf{r} \times \nabla) A_j d^3 r \quad (\text{S3})$$

This gives the gauge independent spin and OAM of electromagnetic wave if Coulomb gauge is chosen in Eq. (S2, S3) [2]. For quasi-monochromatic wave, we can simplify the calculation by using the complex envelope, and note that $E = -i\omega_0 A$. This gives the following expression:

$$\mathbf{L}_{OAM} = \frac{1}{2\mu_0 c^2 \omega_0} \int \text{Re}[E^* \mathbf{r} \times (i\nabla + k_0 \hat{\mathbf{z}}) E] d^3 r \quad (\text{S4})$$

The second term can be regarded as external OAM that arises from the center of mass motion of the pulse. We neglect its contribution in all following calculations. Devide this by the energy U contained in the pulse $U = \frac{\epsilon_0}{2} \int \text{Re}(E^* E) d^3 r$, and note that the OAM operator $\mathbf{r} \times i\nabla$ is Hermitian, we get the following expression for OAM per photon in the pulse:

$$\frac{L_{OAM}}{U} = \frac{\hbar}{\hbar \omega_0} \frac{\int E^* (\mathbf{r} \times i\nabla) E d^3 r}{\int E^* E d^3 r} \quad (\text{S5})$$

We now consider the OAM of a general pulse with nodal line in real space time. We consider a pulse that has the following envelope at a given time:

$$E(x, y, z) = (F_x x + F_y y + F_z z) \exp\left(-\frac{\Delta k_z^2 z^2}{4}\right) \exp\left(-\frac{\Delta k_x^2 x^2}{4}\right) \exp\left(-\frac{\Delta k_y^2 y^2}{4}\right) \quad (\text{S6})$$

Here $F_{x,y,z}$ are arbitrary complex coefficients. Using Eq (S5), we can calculate the OAM per photon of the pulse. The results are:

$$L_x = \frac{\text{Im}(F_z^* F_y) (\Delta k_y^2 + \Delta k_z^2) \Delta k_x^2}{|F_x|^2 \Delta k_y^2 \Delta k_z^2 + |F_y|^2 \Delta k_x^2 \Delta k_z^2 + |F_z|^2 \Delta k_x^2 \Delta k_y^2} \hbar \quad (\text{S7})$$

$$L_y = \frac{\text{Im}(F_x^* F_z) (\Delta k_x^2 + \Delta k_z^2) \Delta k_y^2}{|F_x|^2 \Delta k_y^2 \Delta k_z^2 + |F_y|^2 \Delta k_x^2 \Delta k_z^2 + |F_z|^2 \Delta k_x^2 \Delta k_y^2} \hbar \quad (\text{S8})$$

$$L_z = \frac{\text{Im}(F_y^* F_x) (\Delta k_x^2 + \Delta k_y^2) \Delta k_z^2}{|F_x|^2 \Delta k_y^2 \Delta k_z^2 + |F_y|^2 \Delta k_x^2 \Delta k_z^2 + |F_z|^2 \Delta k_x^2 \Delta k_y^2} \hbar \quad (\text{S9})$$

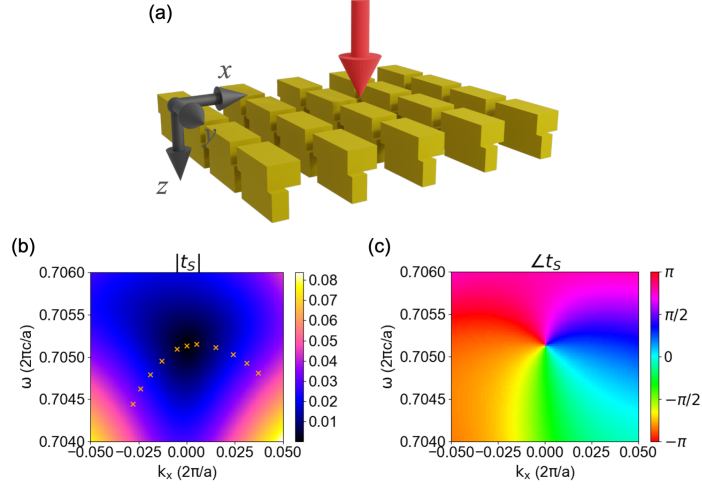


Fig. S1. Demonstration of general transmission nodal line in photonic crystal slab transmission. (a) Schematic of structure (yellow), and incidence pulse (red arrow). The structure has $\epsilon = 12$ and the unit cell is composed of two cubes with x, y, z dimensions $(0.4a, 0.8a, 0.28a)$, $(0.2a, 0.8a, 0.32a)$, with the second cube center displaced by $(-0.1a, 0.1a, 0.3a)$ relative to the first one. (b) Transmission amplitude on the $k_y = 0$ plane. The crosses denote the position of zero on $\omega - k_x$ plane for $k_y = (-0.009, -0.007, -0.005, -0.003, -0.001, 0.0, 0.001, 0.003, 0.005, 0.007, 0.009) \times 2\pi/a$. (c) Phase of transmission on the $k_y = 0$ plane.

This leads us to Eq (7) of the main text. We also see that when the pulse is anisotropic, its OAM value is not quantized, also the direction of its OAM is not the same as the direction of the nodal line.

In the numerical calculation of OAM, the profile in (x, y, t) space is obtained from transmission coefficients. To transform this into the (x, y, z) space, we note that for short propagation distances near the focus (both temporally and spatially), diffraction can be neglected. We simply replace ct with $-z$ to get the pulse profile in real space [3].

Using the pulse profile, we numerically calculate the OAM of the pulse using Eq. (S5). We also calculate the extrinsic OAM by calculating the center of mass motion induced contribution to OAM, and subtract them in the final result of OAM. This helps to get a stable value of OAM, since even for small distortion of the pulse the extrinsic OAM can already have a large contribution compared with the intrinsic one.

2. GENERAL EXISTENCE OF TRANSMISSION NODAL LINE

Here we consider a photonic crystal slab without any symmetry in its unit cell. The structure is shown in Fig. S1a. We calculate its transmission coefficient for y polarized input light. The output polarization is chosen such that cross-polarization condition is satisfied for normal incidence at a specific frequency. This give rise to $t = 0$ at $k_x = 0$ at this chosen frequency. The transmission coefficient in the $k_y = 0$ plane is plotted in Fig. S1b for amplitude and S1c for phase. We see this zero has an associated winding around it. For each $k_y \neq 0$, we can still find a point of zero in transmission in the $\omega - k_y$ plane and we indicate their positions by 'x's in Fig. S1b. We therefore see the existence of a nodal line does not depend on any symmetry in the photonic crystal slab, and here its direction also does not follow any particular high symmetry direction.

3. GRATING WITH Z MIRROR SYMMETRY

Fig. S2a shows the cross section of the grating structure. To understand that the transmission nodal line is pinned on the $k_y = 0$ plane, we show the coupled mode theory model in Fig. S2b. a_{k_x} and a_{-k_x} guided resonances of the slab that are odd in y and couples to four plane wave ports $S_{1,2,3,4}$. These plane waves are all polarized in y . In particular, S_{1+} and S_{3+} couples to a_{k_x} , and a_{k_x} radiates out into S_{2-} and S_{4-} . a_{-k_x} couples to the remaining plane wave modes in a similar way.

In coupled mode theory, all coupling coefficients d_1, d_2, d_3, d_4 are equal due to mirror symmetry along z and reciprocity. Therefore the coupled mode theory equations have the mirror symmetry along x . Thus the nodal line is symmetric in k_x . For the transmission vortex around the nodal line, there is no symmetry here to guarantee the vortex to be isotropic. For an arbitrarily chosen structure within symmetry constraint, Fig. S2c-f shows a highly anisotropic vortex around the nodal line.

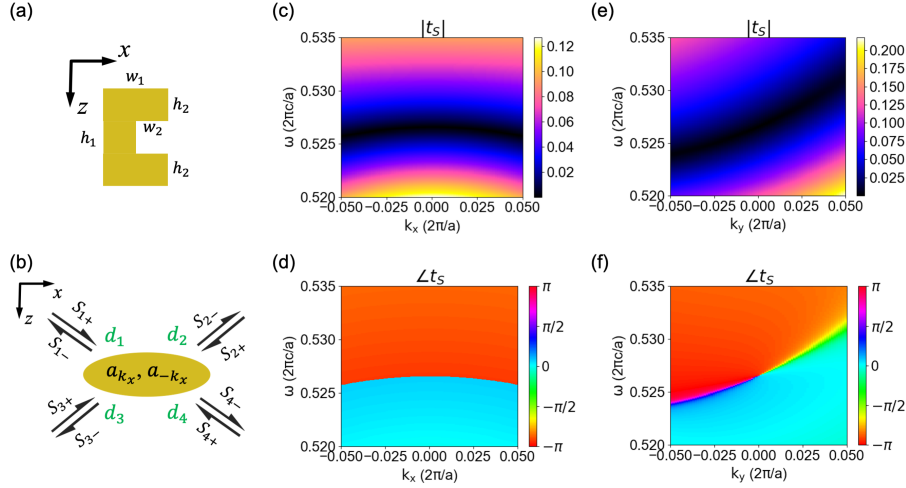


Fig. S2. Transmission coefficient of y polarized input, LCP output for the structure in Fig. 4a. (a) The grating cross section has dimensions $w_1 = 0.4a, w_2 = 0.2a, h_1 = 0.6a, h_2 = 0.2a$. (b) Coupled mode model for the photonic crystal slab. $S_{1,2,3,4}$ are four plane wave ports, with $+$ denoting input and $-$ denoting output of the resonances. a_{k_x} and a_{-k_x} are guided resonances at positive and negative k_x . $d_{1,2,3,4}$ are coupling coefficients of the guided resonances to corresponding ports. They are all equal in this case. (c) amplitude and (d) phase of the transmission coefficient on $k_y = 0$ plane. The nodal line lies on this plane. (e) amplitude and (f) phase of the transmission coefficient on $k_x = 0$ plane.

4. OPTIMIZATION METHOD

In this work, we used optimization method to get a design that has reasonably good performance. We use an autograd implementation of RCWA to simulate the structure and get the gradient with respect to pixel value in the design region [4]. The objective function is defined as follows:

$$\sum_j |(t_{j,\text{sim}} e^{i\delta} - t_{j,\text{obj}}) \cdot w_j|^2 \quad (\text{S10})$$

Here j represents different sample points in (k_x, k_y, ω) space, $t_{j,\text{sim}}$ and $t_{j,\text{obj}}$ represent the simulated and desired transmission function at a particular sample point. δ is a phase factor obtained by equalizing the phase of $t_{j,\text{sim}}$ and $t_{j,\text{obj}}$ at a particular sample point. This alleviates the need for choosing a suitable reference plane. w_j are the weights for each sample point, chosen to be 1 on the $k_x = 0$ plane and 2.5 along the nodal line.

The initial condition for the dielectric permittivity distribution is chosen to be coherent noise [5], which is beneficial for generating low Q resonances in the photonic crystal slab. The objective function in the transmission is chosen as:

$$t(k_x = 0, k_y, \omega) = \frac{6k_y - 65i(\omega - 0.64)}{\sqrt{1 + (6k_y)^2 + [65(\omega - 0.64)]^2}} \quad (\text{S11})$$

$$t(k_x, k_y = 0, \omega = 0.64 + 1.0k_x^2) = 0 \quad (\text{S12})$$

The wavevectors are in units of $2\pi/a$, and angular frequency in units of $2\pi c/a$. The sampling region is $0.635 < \omega < 0.645, |k_y| < 0.05, |k_x| < 0.06$. The specific choice is due to the existence of a vortex structure near $\omega = 0.64$ in the initial structure. The function parameters could change

for different initializations. We use the method of moving asymptote [6] implemented in NLOpt [7] to optimize the permittivity distribution. Binarization is obtained by using an activation function in translating the pixel values to actual permittivity values. Running the optimization algorithm repeatedly with steeper activation function eventually gives a near binarized structure. Despite the optimization algorithm is used, several trials and hand tuning are still needed to get a reasonably performing device.

REFERENCES

1. J. D. Jackson, "Classical electrodynamics," (1999).
2. M. Mansuripur, "Spin and orbital angular momenta of electromagnetic waves in free space," *Phys. Rev. A* **84**, 033838 (2011).
3. A. Chong, C. Wan, J. Chen, and Q. Zhan, "Generation of spatiotemporal optical vortices with controllable transverse orbital angular momentum," *Nat. Photonics* **14**, 350–354 (2020).
4. W. Jin, W. Li, M. Orenstein, and S. Fan, "Inverse design of lightweight broadband reflector for relativistic lightsail propulsion," *ACS Photonics* **7**, 2350–2355 (2020).
5. N. Zhao, P. B. Catrysse, and S. Fan, "Perfect RGB-IR color routers for sub-wavelength size cmos image sensor pixels," *Adv. Photonics Res.* p. 2000048.
6. K. Svanberg, "A class of globally convergent optimization methods based on conservative convex separable approximations," *SIAM journal on optimization* **12**, 555–573 (2002).
7. S. G. Johnson, "The nlopt nonlinear-optimization package," <http://github.com/stevengj/nlopt>.